Orbital and spin character of doped carriers in infinite-layer nickelates

M. Rossi, H. Lu, A. Nag, D. Li, M. Osada, K. Lee, B. Y. Wang, S. Agrestini, M. Garcia-Fernandez, J. J. Kas, Y.-D. Chuang, Z. X. Shen, H. Y. Hwang, B. Moritz, Ke-Jin Zhou, T. P. Devereaux, and W. S. Lee

Phys. Rev. B **104**, L220505 — Published 8 December 2021

DOI: 10.1103/PhysRevB.104.L220505

Orbital and Spin Character of Doped Carriers in Infinite-Layer Nickelates

M. Rossi,[1] H. Lu,[1,2] A. Nag,[3] D. Li,[1,4] M. Osada,[1,5] K. Lee,[1,2] B. Y. Wang,[1,2] S. Agrestini,[3] M. Garcia-Fernandez,[3] J. J. Kas,[6,1] Y.-D. Chuang,[7] Z. X. Shen,[1,2,4,8] H. Y. Hwang,[1,4,8] B. Moritz,[1] Ke-Jin Zhou,[3] T. P. Devereaux,[1,5,8,*] and W. S. Lee[1,†]

[1] *Stanford Institute for Materials and Energy Sciences, SLAC National Accelerator Laboratory, 2575 Sand Hill Road, Menlo Park, California 94025, USA*
[2] *Department of Physics, Stanford University, Stanford, California 94305, USA*
[3] *Diamond Light Source, Harwell Campus, Didcot OX11 0DE, United Kingdom*
[4] *Department of Applied Physics, Stanford University, Stanford, California 94305, USA*
[5] *Department of Materials Science and Engineering, Stanford University, Stanford, California 94305, USA*
[6] *Department of Physics, University of Washington, Seattle, Washington 98195, USA*
[7] *Advanced Light Source, Lawrence Berkeley National Laboratory, 1 Cyclotron Road, MS 6-2100, Berkeley, California 94720, USA*
[8] *Geballe Laboratory for Advanced Materials, Stanford University, Stanford, California 94305, USA*

The recent discovery of superconductivity in $Nd_{1-x}Sr_xNiO_2$ has drawn significant attention in the field. A key open question regards the evolution of the electronic structure with respect to hole doping. Here, we exploit x-ray absorption spectroscopy (XAS) and resonant inelastic x-ray scattering (RIXS) to probe the doping dependent electronic structure of $Nd_{1-x}Sr_xNiO_2$. Upon doping, a high-energy feature in Ni L_3-edge XAS develops in addition to the main absorption peak, while XAS at the O K-, Nd M_3- and Nd M_5-edge exhibits a much weaker response. This implies that doped holes are mainly introduced into Ni $3d$ states. By comparing our data to atomic multiplet calculations including D_{4h} crystal field, the doping induced feature in Ni L_3-edge XAS is consistent with a d^8 spin singlet state, in which doped holes reside in the $3d_{x^2-y^2}$ orbitals. This is further supported by the softening of RIXS orbital excitations upon doping, corroborating with the Fermi level shift associated with increasing holes in the Ni $3d_{x^2-y^2}$ orbital.

Infinite-layer nickelates have been proposed more than two decades ago as promising materials that may host unconventional superconductivity [1]. Inspired by the crystal and electronic structure of high-temperature superconducting cuprates, Anisimov *et al.* [1] investigated $LaNiO_2$ that shares some of their essential characteristics: two-dimensional NiO_2 planes, nominal $3d^9$ valence configuration, and a $3d_{x^2-y^2}$-derived band crossing the Fermi level. However, superconductivity in nickelates remained elusive until very recently, when Li *et al.* reported the first experimental evidence of a zero-resistance state in thin films of $Nd_{0.8}Sr_{0.2}NiO_2$ [2] with a transition temperature around 10 K at optimal doping [3, 4].

Although the early theoretical investigation was motivated by the search for cuprate analogs [1], some differences between the parent compounds of cuprates and nickelates emerge [5]. $NdNiO_2$ is a poor conductor [2] and lacks evidence of long-range magnetic order [6]. Recent x-ray absorption spectroscopy (XAS) and resonant inelastic x-ray scattering (RIXS) experiments [7] have indicated that the charge-transfer energy to the O ligands is large, resulting in a much reduced hybridization between Ni and O states with respect to cuprates and other charge-transfer compounds. Theoretical calculations have suggested that the low energy model involves a Hubbard-like two-dimensional Ni $3d_{x^2-y^2}$ band and a three-dimensional metallic Nd $5d_{3z^2-r^2}$ band [7, 8]. Other calculations propose that additional rare earth $5d$ orbitals might be also relevant near the Fermi energy [8–18]. While further experimental scrutiny is required, an emerging consensus is that multi-orbital physics likely plays an important role in the electronic structure of the parent compounds of infinite-layer nickelates.

Since superconductivity emerges in $NdNiO_2$ when trivalent Nd is substituted by divalent Sr [2–4], it is important to establish the evolution of the electronic structure upon doping. To date, theories have proposed distinct scenarios that depend on the interplay between electronic correlation, charge-transfer energy, crystal field splitting and Hunds coupling [14, 19–23]. For example, doped holes may give rise to Ni $3d^8$ sites, where the two holes may arrange in a singlet (double occupation of $3d_{x^2-y^2}$ orbital) [1, 24–27] or triplet (occupation of different orbitals) [28–31] configuration; or they may form $d^9\underline{L}$ states (where $\underline{L}$ denotes a hole in the O $2p$ orbitals) that resemble Zhang-Rice singlets [32] typical of doped cuprates [33]; also, carriers may be introduced into the Nd $5d$ states [22, 34]. Experimental determination of the orbital and spin character of doped holes is therefore highly desirable to clarify this issue.

Notably, using electron energy loss spectroscopy (EELS), Goodge *et al.* [35] recently reported changes in the absorption spectra of $Nd_{1-x}Sr_xNiO_2$ at the O, Ni and Nd edges, suggesting that doped carriers appear to reside primarily on Ni sites forming d^8 states with little change in oxygen content – much less than that observed

* Corresponding author: tpd@stanford.edu
† Corresponding author: leews@stanford.edu

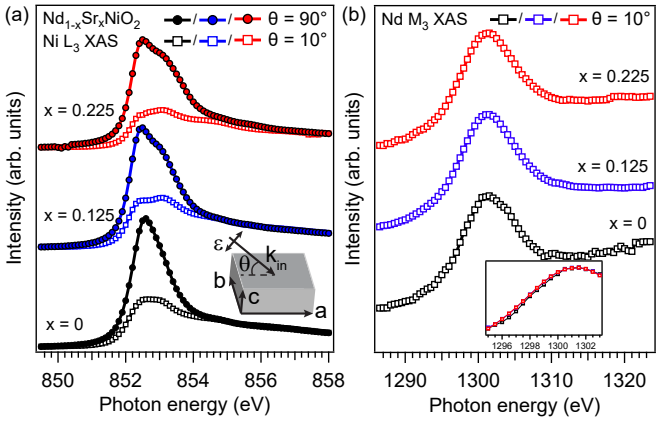

FIG. 1. (a) Total electron yield Ni L_3-edge XAS of $Nd_{1-x}Sr_xNiO_2$. A constant background has been removed and the post-edge intensity has been set to 1. The drawing shows the direction of the photon polarization $\boldsymbol{\epsilon}$ in the sample reference frame *abc*. (b) Total electron yield Nd M_3-edge XAS. A constant background has been removed and the peak intensity has been set to 1 for better comparison of the peak region. The inset zooms into the energy range corresponding to the leading edge.

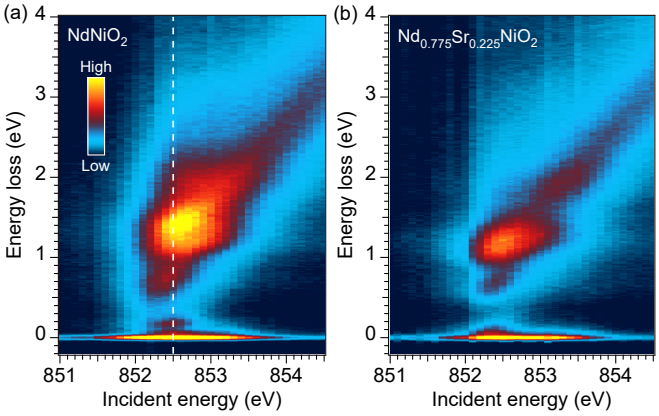

FIG. 2. RIXS intensity maps of $NdNiO_2$ (a) and $Nd_{0.775}Sr_{0.225}NiO_2$ (b) as a function of incident photon energy across the Ni L_3 edge. RIXS spectra were collected at an incidence angle of 35° and scattering angle of 154°. The dashed line marks the incident energy selected for the measurement of the angular dependence of RIXS spectra. Data reported in panel (a) are taken from Ref. 38.

in cuprates [36]. Yet, further spectroscopic studies are needed to confirm these results, establish whether the two holes in the Ni 3*d* states arrange in a singlet or triplet configuration, and determine the role of the Nd 5*d* states.

In this Letter, we use a combination of high-resolution XAS and RIXS and multiplet calculations to investigate the orbital and spin states of doped holes in $Nd_{1-x}Sr_xNiO_2$. We consider three doping levels: $x = 0$ (undoped), 0.125 (non-superconducting), and 0.225 (superconducting, $T_c \approx 10$ K). XAS and RIXS are suitable techniques for our purpose since the resonant excitation grants element selectivity while enhancing the scattering cross-section, which is crucial for thin film samples. We find that doped holes are primarily introduced in the Ni $3d_{x^2-y^2}$ Hubbard band in a low-spin configuration associated with a shift of Fermi level that is reflected in the softening of orbital excitations by approximately 0.2 eV between compounds with Sr content of $x = 0$ and 0.225.

Thin films of the precursor perovskite $Nd_{1-x}Sr_xNiO_3$ with a thickness of 10 nm were grown on a substrate of $SrTiO_3$(001). The *c*-axis oriented infinite-layer $Nd_{1-x}Sr_xNiO_2$ was obtained by means of a topotactic reduction process [37]. To protect and support the crystalline order, a capping layer made of five unit cells of $SrTiO_3$(001) was grown on top of the nickelate film. XAS and RIXS measurements were performed at beamline I21 of the Diamond Light Source (United Kingdom). The combined energy resolution of the beamline and the spectrometer was approximately 40 meV at the Ni L_3 edge. Measurements were taken at 20 K. RIXS spectra are normalized to the incident photon flux.

We first study the doping evolution of the electronic states of $Nd_{1-x}Sr_xNiO_2$ by examining XAS spectra at relevant Ni, Nd, and O absorption edges. Figure 1(a) shows Ni L_3-edge XAS spectra taken with two different light polarizations $\boldsymbol{\epsilon}$ set by the incidence angle θ (see inset for a sketch of the experimental geometry). The XAS spectrum of $NdNiO_2$ measured with $\theta = 90°$ ($\boldsymbol{\epsilon} \parallel a$) shows one dominant peak attributed to the $2p^63d^9 \rightarrow 2p^53d^{10}$ transition [7, 35]. Upon doping, XAS spectra measured with $\boldsymbol{\epsilon} \parallel a$ develop an additional shoulder at higher energy than the main peak. This spectral feature is consistent with the broadening of the main absorption peak reported in EELS measurements [35], but is unambiguously resolved in our high-resolution data. For the XAS taken at $\theta = 10°$ ($\boldsymbol{\epsilon}$ mostly along the *c* axis), we observe a strong linear dichroism, suggesting a pronounced in-plane orientation of the unoccupied 3*d* orbitals.

Next, we examine the doping evolution of the Nd 5*d* orbitals, which contribute to the near Fermi energy states in the parent compound. The Nd M_3-edge XAS ($3p \rightarrow 5d$ transition) of $NdNiO_2$ consists of a single broad peak (Fig. 1(b)) that arises from the mostly unoccupied Nd 5*d* states. This is supported by theoretical calculations reported in the Supplemental Material (SM) [39] (see, also, references [1-15] therein). Upon doping, we observe a slight increase of spectral intensity in the leading edge (see inset) from $x = 0$ to 0.125, while there is no clear difference in the spectra between $x = 0.125$ and 0.225. This suggests that the Nd 5d orbitals play a minor role in hosting doped holes, consistent with the small Nd 5*d* electron pockets in the parent compounds predicted in some calculations [5, 8, 11, 17].

XAS spectra of $Nd_{1-x}Sr_xNiO_2$ measured at the O *K* edge ($1s \rightarrow 2p$ transition, see SM [39] and references [1-15] therein) do not reveal the emergence of a pre-peak usually associated with hole doping into the charge-

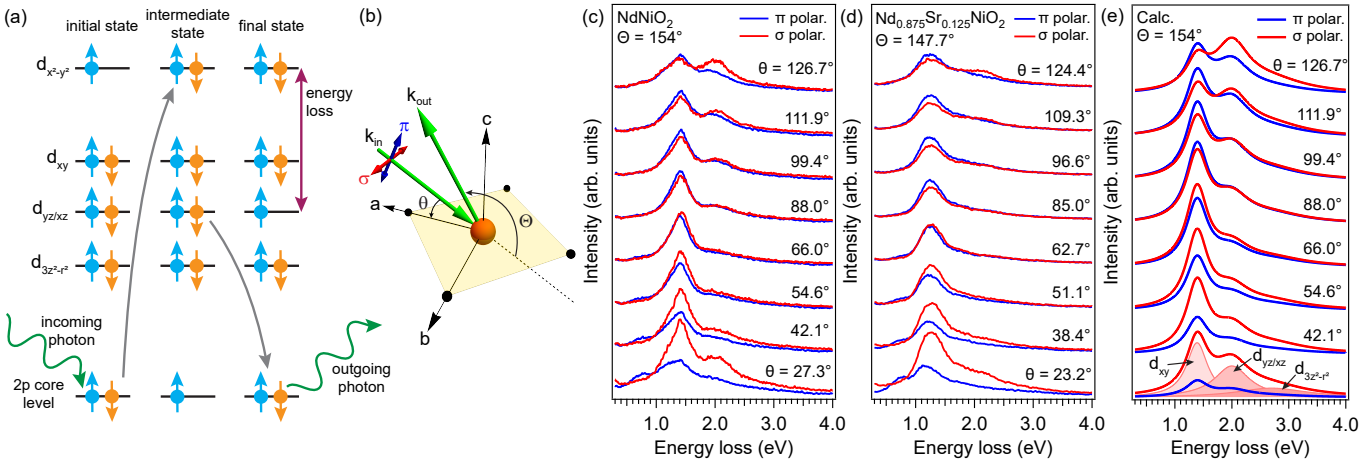

FIG. 3. (a) Schematics of the RIXS process at the Ni L_3 edge. (b) Ni cation (orange sphere) surrounded by O anions (black spheres) and sketch of the experimental geometry. The incoming photon wave vector $\mathbf{k}_{\rm in}$ forms an angle θ with the sample ab plane. The scattered photon wave vector $\mathbf{k}_{\rm out}$ forms an angle Θ with $\mathbf{k}_{\rm in}$. The incident photon polarization is either parallel (π) or perpendicular (σ) to the scattering plane, which coincides with the ac plane. (c, d) Stack plot of RIXS spectra of $NdNiO_2$ (c) and $Nd_{0.875}Sr_{0.125}NiO_2$ (d) collected at various incidence angles θ and fixed scattering angle Θ. The incident energy was fixed to 852.5 eV for $NdNiO_2$ (dashed line in Fig. 2(a)) and 852.44 eV for $Nd_{0.875}Sr_{0.125}NiO_2$. (e) Angular dependence of the intensity of dd transitions calculated for the angles of panel (c).

transfer band [36]. While the signal from the $SrTiO_3$ capping layer could obscure the absorption from the underlying nickelate film, our results nonetheless suggest that the doping induced signature in O K-edge XAS is minor, as confirmed by the spatially-resolved EELS measurements [35]. The Nd M_5-edge XAS spectra ($3d \rightarrow 4f$ transition) are also unaffected by doping (see SM [39] and references [1-15] therein), implying well-localized Nd $4f$ states.

After establishing that doped holes are introduced primarily into Ni $3d$ orbitals, we further analyze the energetics of $3d$ states and their doping dependence using RIXS. Figure 2 displays the RIXS intensity maps of $NdNiO_2$ (a) and $Nd_{0.775}Sr_{0.225}NiO_2$ (b) as a function of incident photon energy across the Ni L_3 edge. The most intense excitations are found at an energy loss of 1–3 eV, which is the typical energy range of crystal field (dd) transitions [40–44]. At an energy loss of ≈ 0.7 eV, an excitation is visible in both compounds. This feature is specific to infinite-layer nickelates and has been attributed to the hybridization between Ni and Nd orbitals [7]. For incident photon energies above 853 eV, a fluorescence-like excitation is observed. Low energy-loss excitations below 0.3 eV will be discussed in separate works [38].

We focus on the dd transitions that carry direct information about the Ni $3d$ orbitals. The energy and orbital character of the dd excitations are analyzed using an ionic model including crystal field. Although simple, the model has proven successful to characterize the orbital excitations of cuprates [42]. We consider a single Ni^+ cation surrounded by four negative point charges in square planar geometry. The D_{4h} tetragonal symmetry of the crystal field lifts the degeneracy of the Ni $3d$ orbitals such that the $d_{3z^2-r^2}$ becomes the lowest energy state, followed by $d_{yz/xz}$, d_{xy} and $d_{x^2-y^2}$. In the L_3-edge RIXS process, illustrated in Fig. 3(a), a $2p_{3/2}$ core electron is first promoted into the empty $3d_{x^2-y^2}$ orbital, then a $3d$ electron radiatively decays producing an electronic redistribution within the $3d$ shell that gives rise to dd transitions in the RIXS spectra. Since the $3d$ orbitals have distinct spatial symmetry, their orientation relative to the polarization vectors of the incident and scattered photons produces a modulation of the RIXS matrix elements and therefore of the dd intensity. Indeed, as shown in Figs. 3(c,d), while the energy and width of the dd excitations of a particular sample do not exhibit notable variation, the relative intensity varies as a function of the incidence angle θ, which effectively alters the polarization direction relative to the orbital orientation (see the sketch of the experimental geometry in Fig. 3(b)). This variation can be used to determine the orbital character of the dd excitations and verify whether the $3d$ energy levels follow the expected D_{4h} crystal field splitting.

We calculate the RIXS cross section of dd transitions using the single ion model, following Ref. 42, which is also described in the SM [39] (see also references [1-15] therein). We considered the incidence and scattering angles reported in Fig. 3(c), but the calculations equally apply to panel (d) since the minor differences in the two experimental geometries do not appreciably affect the dd intensity modulation. The cross sections, reported in panel (e), not only qualitatively reproduce the angular dependence of the experimental intensity for a given incident polarization, but also capture the relative modulation between π and σ polarizations at a given angle. This agreement allows us to attribute the peaks in the RIXS spectra of $NdNiO_2$ at 1.39 and 2.0 eV and the broad tail centered at 2.7 eV to transitions into the d_{xy}, $d_{yz/xz}$, and

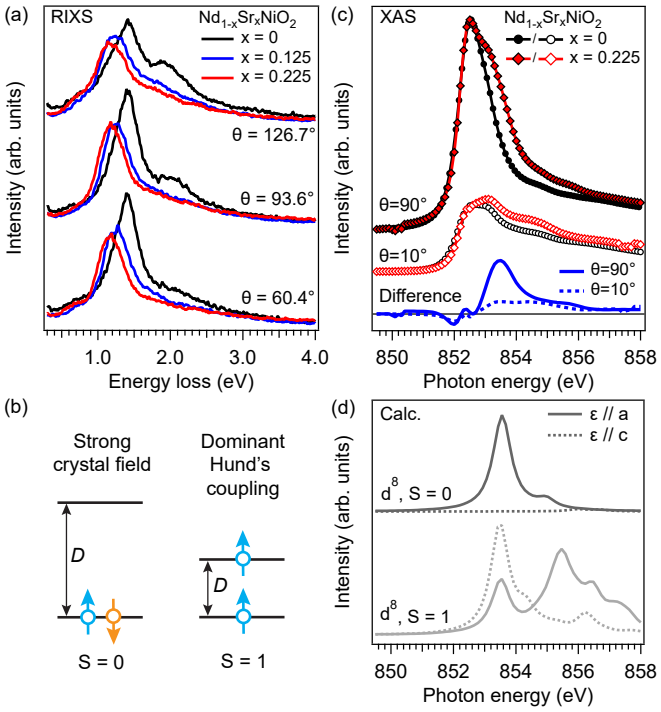

FIG. 4. (a) Doping dependence of the RIXS spectra of $Nd_{1-x}Sr_xNiO_2$ measured at various incidence angles with $\Theta = 154°$ and π incident photon polarization. (b) Two-level diagrams showing the competition between Hund's coupling and crystal field splitting D. (c) XAS spectra of $NdNiO_2$ (black dots) and $Nd_{0.775}Sr_{0.225}NiO_2$ (red diamonds) measured at $\theta = 90°$ ($\boldsymbol{\epsilon} \parallel a$, filled markers) and $\theta = 10°$ ($\boldsymbol{\epsilon}$ almost parallel to c, empty marker). The spectra of the undoped compound are scaled and shifted to match the main peak of the doped sample. The difference between the spectra of $Nd_{0.775}Sr_{0.225}NiO_2$ and $NdNiO_2$ are plotted as blue lines. (d) Multiplet calculations of a d^8 site in spin-singlet ($S = 0$, dark grey) and spin-triplet ($S = 1$, light grey) configuration, respectively. Solid and dotted lines correspond to light polarization parallel to the a and c axes, respectively.

$d_{3z^2-r^2}$ orbitals, respectively, as shown in panel (e). A similar assignment can be made for $Nd_{0.875}Sr_{0.125}NiO_2$. We note that the weaker cross section of the $d_{3z^2-r^2}$ excitation and its larger width compared to other dd transitions prevent us from precisely constrain its energy position. Nevertheless, our assignment is in very good agreement with recent ab initio calculations of $NdNiO_2$ [45] and with experimental and theoretical findings on $CaCuO_2$ [42, 46, 47] and Nd_2CuO_4 [48] that possess the same square planar environment around the d^9 ion. Though, the dd excitation peaks are broader than those of undoped cuprates and appear to deviate from a simple Gaussian or Lorentzian lineshape. These discrepancies may be due to the coupling to the particle-hole excitation continuum of the metallic state of $Nd_{1-x}Sr_xNiO_2$, and to the disorder associated with possible incomplete chemical reduction [35, 37].

We now explore the evolution of orbital excitations upon doping. Figure 4(a) shows the RIXS spectra of three samples with doping of $x = 0$ (black), 0.125 (blue), and 0.225 (red) collected at three representative incidence angles. With increasing doping, the dd excitations are broadened and, most importantly, softened by approximately 0.2 eV at $x = 0.225$. We note that the doping evolution of the dd transitions is distinct from the case of hole-doped cuprates, where dd excitations are broadened upon doping but their center of mass is little influenced [49]. This is because holes are doped into the O-derived charge-transfer band, which induces little effects in the energetics of the Cu $3d$ manifold. Conversely, in electron-doped cuprates the dd excitations harden upon doping. This has been considered as a signature of electron doping into the Cu-derived upper Hubbard band, which effectively increases the energy difference between the Fermi level in $3d_{x^2-y^2}$ band and other filled $3d$ orbitals [50]. Similarly, the softening of the dd excitations in hole-doped infinite-layer nickelates indicates that doped carriers are introduced into the Ni $3d_{x^2-y^2}$ band corroborating with the shift of Fermi level toward the occupied $3d$ orbitals due to injection of holes.

What is the electronic state of doped holes on Ni sites? Depending on the competition between crystal field splitting of the lowest energy $3d$ orbitals and Hund's rule coupling, doped holes on Ni sites (*i.e.* a d^8 state) can arrange either in a spin singlet or triplet configuration, as exemplified in the two-level diagrams of Fig. 4(b). A large Hund's exchange J_H promotes the population of different orbitals in a high-spin state to minimize Coulomb repulsion (right diagram); instead, a strong crystal field D favors a large orbital polarization where holes fill the first available state in a low-spin configuration (left diagram). To shed light on which scenario resembles the doped nickelates, we first extract the doping-induced change in the unoccupied states probed by Ni L_3-edge XAS. Figure 4(c) displays XAS spectra of $NdNiO_2$ (black) and $Nd_{0.775}Sr_{0.225}NiO_2$ (red) measured with $\boldsymbol{\epsilon} \parallel a$ ($\theta = 90°$) and $\boldsymbol{\epsilon}$ mostly along the c axis ($\theta = 10°$). Assuming that the main peak in both compounds originates from the $2p^63d^9 \rightarrow 2p^53d^{10}$ transition, the spectrum of $NdNiO_2$ for $\theta = 90°$ is scaled and shifted by -0.05 eV to match the position and height of the first peak of $Nd_{0.775}Sr_{0.225}NiO_2$. The difference of the two spectra (blue lines) represents the additional contribution generated by doping; it mainly consists of a single peak that is strongly reduced when the polarization is mostly out of plane. Next, we calculate the multiplet spectrum of the d^8 ion in tetragonal crystal field in the two regimes, corresponding to spin triplet and spin singlet states. The parameters used, reported in the SM [39] (see also references [1-15] therein), are set to demonstrate the XAS gross features for the two respective scenarios which are robust against fine tuning. The multiplet spectra of the high- and low-spin states (Fig. 4(d)) have distinct characteristics: the former is made of multiple peaks with similar weight over a wide energy range (light grey). When $\boldsymbol{\epsilon} \parallel c$, the first peak is enhanced, while the intensity of

the high-energy features is reduced. Conversely, the multiplet spectrum of the spin-singlet configuration (dark grey) is dominated by a single peak that is strongly suppressed with out-of-plane polarization. Thus, the spin-singlet scenario where the doped hole occupies the $d_{x^2-y^2}$ orbital agrees with our data.

In conclusion, our results indicate that while the changes in O $2p$, Nd $5d$ and Nd $4f$ states are relatively insignificant, the pronounced doping evolution of the Ni $3d$ orbitals in infinite-layer nickelates is reminiscent of doping a Hubbard band; namely, the doped holes primarily reside in the $d_{x^2-y^2}$ orbital forming a d^8 spin singlet state. Although a low spin configuration is highly uncommon for d^8 nickel compounds, it may become energetically favorable when the Ni ion is embedded in a low-symmetry environment, such as in planar complex K_2Ni-dithio-oxalate [51], trilayer $(La,Pr)_4Ni_3O_8$ [52] and Ni-doped one-dimensional cuprates [53, 54]. Our results imply that the low-energy electronic properties of $Nd_{1-x}Sr_xNiO_2$ are likely dominated by the Ni $3d_{x^2-y^2}$ orbitals. Note that the sign change of the Hall coefficient with temperature and doping [3, 4] has been interpreted as the contribution from multiple bands. However, a similar behavior is also observed in cuprates where a single band description is well established. The complex dependence of the Hall coefficient may be related to electron correlations that influence the topology of the Fermi surface [55–57]. Yet, we emphasize that our observation of dominant Ni $3d_{x^2-y^2}$ states does not exclude the possible existence of remnants of Nd $5d$ Fermi pockets in the doped compounds. If so, the weak doping dependence of these orbitals may suggest a more complex doping evolution than a simple rigid band shift, which remains an interesting open question.

ACKNOWLEDGMENTS

We are grateful to G. A. Sawatzky for stimulating discussions. This work is supported by the U.S. Department of Energy (DOE), Office of Science, Basic Energy Sciences, Materials Sciences and Engineering Division, under contract DE-AC02-76SF00515. We acknowledge the Gordon and Betty Moore Foundations Emergent Phenomena in Quantum Systems Initiative through grant number GBMF4415 for synthesis equipment. We acknowledge Diamond Light Source for time on beamline I21-RIXS under Proposal NT25165 and MM25598. This research also used resources of the Advanced Light Source, a U.S. DOE Office of Science User Facility under contract no. DE-AC02-05CH11231.

[1] V. I. Anisimov, D. Bukhvalov, and T. M. Rice, Electronic structure of possible nickelate analogs to the cuprates, Phys. Rev. B **59**, 7901 (1999).
[2] D. Li, K. Lee, B. Y. Wang, M. Osada, S. Crossley, H. R. Lee, Y. Cui, Y. Hikita, and H. Y. Hwang, Superconductivity in an infinite-layer nickelate, Nature **572**, 624 (2019).
[3] D. Li, B. Y. Wang, K. Lee, S. P. Harvey, M. Osada, B. H. Goodge, L. F. Kourkoutis, and H. Y. Hwang, Superconducting Dome in $Nd_{1-x}Sr_xNiO_2$ Infinite Layer Films, Phys. Rev. Lett. **125**, 027001 (2020).
[4] S. Zeng, C. S. Tang, X. Yin, C. Li, M. Li, Z. Huang, J. Hu, W. Liu, G. J. Omar, H. Jani, Z. S. Lim, K. Han, D. Wan, P. Yang, S. J. Pennycook, A. T. S. Wee, and A. Ariando, Phase Diagram and Superconducting Dome of Infinite-Layer $Nd_{1-x}Sr_xNiO_2$ Thin Films, Phys. Rev. Lett. **125**, 147003 (2020).
[5] K.-W. Lee and W. E. Pickett, Infinite-layer $LaNiO_2$: Ni^{1+} is not Cu^{2+}, Phys. Rev. B **70**, 165109 (2004).
[6] M. Hayward and M. Rosseinsky, Synthesis of the infinite layer Ni(I) phase $NdNiO_{2+x}$ by low temperature reduction of $NdNiO_3$ with sodium hydride, Solid State Sci. **5**, 839 (2003).
[7] M. Hepting, D. Li, C. J. Jia, H. Lu, E. Paris, Y. Tseng, X. Feng, M. Osada, E. Been, Y. Hikita, Y.-D. Chuang, Z. Hussain, K. J. Zhou, A. Nag, M. Garcia-Fernandez, M. Rossi, H. Y. Huang, D. J. Huang, Z. X. Shen, T. Schmitt, H. Y. Hwang, B. Moritz, J. Zaanen, T. P. Devereaux, and W. S. Lee, Electronic structure of the parent compound of superconducting infinite-layer nickelates, Nat. Mater. **19**, 381 (2020).
[8] E. Been, W.-S. Lee, H. Y. Hwang, Y. Cui, J. Zaanen, T. Devereaux, B. Moritz, and C. Jia, Electronic Structure Trends Across the Rare-Earth Series in Superconducting Infinite-Layer Nickelates, Phys. Rev. X **11**, 011050 (2021).
[9] Y. Nomura, M. Hirayama, T. Tadano, Y. Yoshimoto, K. Nakamura, and R. Arita, Formation of a two-dimensional single-component correlated electron system and band engineering in the nickelate superconductor $NdNiO_2$, Phys. Rev. B **100**, 205138 (2019).
[10] P. Adhikary, S. Bandyopadhyay, T. Das, I. Dasgupta, and T. Saha-Dasgupta, Orbital-selective superconductivity in a two-band model of infinite-layer nickelates, Phys. Rev. B **102**, 100501(R) (2020).
[11] A. S. Botana and M. R. Norman, Similarities and Differences between $LaNiO_2$ and $CaCuO_2$ and Implications for Superconductivity, Phys. Rev. X **10**, 011024 (2020).
[12] Y. Gu, S. Zhu, X. Wang, J. Hu, and H. Chen, A substantial hybridization between correlated Ni-d orbital and itinerant electrons in infinite-layer nickelates, Commun. Phys. **3**, 84 (2020).
[13] J. Kapeghian and A. S. Botana, Electronic structure and magnetism in infinite-layer nickelates $RNiO_2$ (R = La−Lu), Phys. Rev. B **102**, 205130 (2020).
[14] F. Lechermann, Late transition metal oxides with infinite-layer structure: Nickelates versus cuprates, Phys. Rev. B **101**, 081110 (2020).
[15] I. Leonov, S. L. Skornyakov, and S. Y. Savrasov, Lifshitz transition and frustration of magnetic moments in infinite-layer $NdNiO_2$ upon hole doping, Phys. Rev. B **101**, 241108 (2020).

[16] Z. Liu, Z. Ren, W. Zhu, Z. Wang, and J. Yang, Electronic and magnetic structure of infinite-layer $NdNiO_2$: trace of antiferromagnetic metal, npj Quantum Mater. **5**, 31 (2020).

[17] H. Sakakibara, H. Usui, K. Suzuki, T. Kotani, H. Aoki, and K. Kuroki, Model Construction and a Possibility of Cupratelike Pairing in a New d^9 Nickelate Superconductor $(Nd, Sr)NiO_2$, Phys. Rev. Lett. **125**, 077003 (2020).

[18] X. Wu, D. Di Sante, T. Schwemmer, W. Hanke, H. Y. Hwang, S. Raghu, and R. Thomale, Robust $d_{x^2-y^2}$-wave superconductivity of infinite-layer nickelates, Phys. Rev. B **101**, 060504 (2020).

[19] L.-H. Hu and C. Wu, Two-band model for magnetism and superconductivity in nickelates, Phys. Rev. Research **1**, 032046 (2019).

[20] M. Jiang, M. Berciu, and G. A. Sawatzky, Critical nature of the ni spin state in doped ndnio$_2$, Phys. Rev. Lett. **124**, 207004 (2020).

[21] Z. Liu, C. Xu, C. Cao, W. Zhu, Z. F. Wang, and J. Yang, Doping dependence of electronic structure of infinite-layer $NdNiO_2$, Phys. Rev. B **103**, 045103 (2021).

[22] F. Petocchi, V. Christiansson, F. Nilsson, F. Aryasetiawan, and P. Werner, Normal State of $Nd_{1-x}Sr_xNiO_2$ from Self-Consistent GW + EDMFT, Phys. Rev. X **10**, 041047 (2020).

[23] X. Wan, V. Ivanov, G. Resta, I. Leonov, and S. Y. Savrasov, Exchange interactions and sensitivity of the Ni two-hole spin state to Hund's coupling in doped $NdNiO_2$, Phys. Rev. B **103**, 075123 (2021).

[24] M. Kitatani, L. Si, O. Janson, R. Arita, Z. Zhong, and K. Held, Nickelate superconductors – a renaissance of the one-band Hubbard model, npj Quantum Mater. **5**, 59 (2020).

[25] H. Zhang, L. Jin, S. Wang, B. Xi, X. Shi, F. Ye, and J.-W. Mei, Effective Hamiltonian for nickelate oxides $Nd_{1-x}Sr_xNiO_2$, Phys. Rev. Research **2**, 013214 (2020).

[26] G.-M. Zhang, Y.-f. Yang, and F.-C. Zhang, Self-doped Mott insulator for parent compounds of nickelate superconductors, Phys. Rev. B **101**, 020501(R) (2020).

[27] J. Krishna, H. LaBollita, A. O. Fumega, V. Pardo, and A. S. Botana, Effects of Sr doping on the electronic and spin-state properties of infinite-layer nickelates: Nature of holes, Phys. Rev. B **102**, 224506 (2020).

[28] J. Chang, J. Zhao, and Y. Ding, Hund-Heisenberg model in superconducting infinite-layer nickelates, Eur. Phys. J. B **93**, 220 (2020).

[29] F. Lechermann, Multiorbital Processes Rule the $Nd_{1-x}Sr_xNiO_2$ Normal State, Phys. Rev. X **10**, 041002 (2020).

[30] P. Werner and S. Hoshino, Nickelate superconductors: Multiorbital nature and spin freezing, Phys. Rev. B **101**, 041104 (2020).

[31] Y.-H. Zhang and A. Vishwanath, Type-II $t-J$ model in superconducting nickelate $Nd_{1-x}Sr_xNiO_2$, Phys. Rev. Research **2**, 023112 (2020).

[32] Z.-J. Lang, R. Jiang, and W. Ku, Strongly correlated doped hole carriers in the superconducting nickelates: Their location, local many-body state, and low-energy effective Hamiltonian, Phys. Rev. B **103**, L180502 (2021).

[33] F. C. Zhang and T. M. Rice, Effective Hamiltonian for the superconducting Cu oxides, Phys. Rev. B **37**, 3759 (1988).

[34] M.-Y. Choi, K.-W. Lee, and W. E. Pickett, Role of $4f$ states in infinite-layer $NdNiO_2$, Phys. Rev. B **101**, 020503 (2020).

[35] B. H. Goodge, D. Li, K. Lee, M. Osada, B. Y. Wang, G. A. Sawatzky, H. Y. Hwang, and L. F. Kourkoutis, Doping evolution of the mott–hubbard landscape in infinite-layer nickelates, Proc. Natl. Acad. Sci. USA **118**, 10.1073/pnas.2007683118 (2021).

[36] C. T. Chen, F. Sette, Y. Ma, M. S. Hybertsen, E. B. Stechel, W. M. C. Foulkes, M. Schulter, S.-W. Cheong, A. S. Cooper, L. W. Rupp, B. Batlogg, Y. L. Soo, Z. H. Ming, A. Krol, and Y. H. Kao, Electronic states in $La_{2-x}Sr_xCuO_{4+\delta}$ probed by soft-x-ray absorption, Phys. Rev. Lett. **66**, 104 (1991).

[37] K. Lee, B. H. Goodge, D. Li, M. Osada, B. Y. Wang, Y. Cui, L. F. Kourkoutis, and H. Y. Hwang, Aspects of the synthesis of thin film superconducting infinite-layer nickelates, APL Mater. **8**, 041107 (2020).

[38] H. Lu, M. Rossi, A. Nag, M. Osada, D. F. Li, K. Lee, B. Y. Wang, M. Garcia-Fernandez, S. Agrestini, Z. X. Shen, E. M. Been, B. Moritz, T. P. Devereaux, J. Zaanen, H. Y. Hwang, K.-J. Zhou, and W. S. Lee, Magnetic excitations in infinite-layer nickelates, Science **373**, 213 (2021).

[39] See Supplemental Material for additional data and details on the calculations.

[40] G. Ghiringhelli, N. B. Brookes, E. Annese, H. Berger, C. Dallera, M. Grioni, L. Perfetti, A. Tagliaferri, and L. Braicovich, Low Energy Electronic Excitations in the Layered Cuprates Studied by Copper L_3 Resonant Inelastic X-Ray Scattering, Phys. Rev. Lett. **92**, 117406 (2004).

[41] G. Ghiringhelli and M. Matsubara and C. Dallera and F. Fracassi and R. Gusmeroli and A. Piazzalunga and A. Tagliaferri and N. B. Brookes and A. Kotani and L. Braicovich, NiO as a test case for high resolution resonant inelastic soft x-ray scattering, J. Phys. Condens. Matter **17**, 5397 (2005).

[42] M. M. Sala, V. Bisogni, C. Aruta, G. Balestrino, H. Berger, N. B. Brookes, G. M. de Luca, D. D. Castro, M. Grioni, M. Guarise, P. G. Medaglia, F. M. Granozio, M. Minola, P. Perna, M. Radovic, M. Salluzzo, T. Schmitt, K. J. Zhou, L. Braicovich, and G. Ghiringhelli, Energy and symmetry of dd excitations in undoped layered cuprates measured by Cu L_3 resonant inelastic x-ray scattering, New J. Phys. **13**, 043026 (2011).

[43] V. Bisogni, S. Catalano, R. J. Green, M. Gibert, R. Scherwitzl, Y. Huang, V. N. Strocov, P. Zubko, S. Balandeh, J.-M. Triscone, G. Sawatzky, and T. Schmitt, Ground-state oxygen holes and the metalinsulator transition in the negative charge-transfer rare-earth nickelates, Nat. Commun. **7**, 13017 (2016).

[44] G. Fabbris, D. Meyers, L. Xu, V. M. Katukuri, L. Hozoi, X. Liu, Z.-Y. Chen, J. Okamoto, T. Schmitt, A. Uldry, B. Delley, G. D. Gu, D. Prabhakaran, A. T. Boothroyd, J. van den Brink, D. J. Huang, and M. P. M. Dean, Doping Dependence of Collective Spin and Orbital Excitations in the Spin-1 Quantum Antiferromagnet $La_{2-x}Sr_xNiO_4$ Observed by X Rays, Phys. Rev. Lett. **118**, 156402 (2017).

[45] V. M. Katukuri, N. A. Bogdanov, O. Weser, J. van den Brink, and A. Alavi, Electronic correlations and magnetic interactions in infinite-layer $NdNiO_2$, Phys. Rev. B **102**, 241112(R) (2020).

[46] M. Minola, L. Hozoi, D. Di Castro, R. Felici, M. Moretti Sala, A. Tebano, G. Balestrino, G. Ghir-

inghelli, J. van den Brink, and L. Braicovich, Measurement of the effect of lattice strain on magnetic interactions and orbital splitting in $CaCuO_2$ using resonant inelastic x-ray scattering, Phys. Rev. B **87**, 085124 (2013).

[47] L. Hozoi, L. Siurakshina, P. Fulde, and J. van den Brink, Ab Initio determination of Cu 3d orbital energies in layered copper oxides, Sci. Rep. **1**, 65 (2011).

[48] M. Kang, J. Pelliciari, Y. Krockenberger, J. Li, D. E. McNally, E. Paris, R. Liang, W. N. Hardy, D. A. Bonn, H. Yamamoto, T. Schmitt, and R. Comin, Resolving the nature of electronic excitations in resonant inelastic x-ray scattering, Phys. Rev. B **99**, 045105 (2019).

[49] R. Fumagalli, L. Braicovich, M. Minola, Y. Y. Peng, K. Kummer, D. Betto, M. Rossi, E. Lefrançois, C. Morawe, M. Salluzzo, H. Suzuki, F. Yakhou, M. Le Tacon, B. Keimer, N. B. Brookes, M. M. Sala, and G. Ghiringhelli, Polarization-resolved Cu L_3-edge resonant inelastic x-ray scattering of orbital and spin excitations in $NdBa_2Cu_3O_{7-\delta}$, Phys. Rev. B **99**, 134517 (2019).

[50] M. Hepting, L. Chaix, E. W. Huang, R. Fumagalli, Y. Y. Peng, B. Moritz, K. Kummer, N. B. Brookes, W. C. Lee, M. Hashimoto, T. Sarkar, J.-F. He, C. R. Rotundu, Y. S. Lee, R. L. Greene, L. Braicovich, G. Ghiringhelli, Z. X. Shen, T. P. Devereaux, and W. S. Lee, Three-dimensional collective charge excitations in electron-doped copper oxide superconductors, Nature **563**, 374 (2018).

[51] G. van der Laan, B. T. Thole, G. A. Sawatzky, and M. Verdaguer, Multiplet structure in the $L_{2,3}$ x-ray-absorption spectra: A fingerprint for high- and low-spin Ni^{2+} compounds, Phys. Rev. B **37**, 6587(R) (1988).

[52] J. Zhang, A. S. Botana, J. W. Freeland, D. Phelan, H. Zheng, V. Pardo, M. R. Norman, and J. F. Mitchell, Large orbital polarization in a metallic square-planar nickelate, Nat. Phys. **13**, 864 (2017).

[53] Y. Utz, F. Hammerath, R. Kraus, T. Ritschel, J. Geck, L. Hozoi, J. van den Brink, A. Mohan, C. Hess, K. Karmakar, S. Singh, D. Bounoua, R. Saint-Martin, L. Pinsard-Gaudart, A. Revcolevschi, B. Büchner, and H.-J. Grafe, Effect of different in-chain impurities on the magnetic properties of the spin chain compound $SrCuO_2$ probed by NMR, Phys. Rev. B **96**, 115135 (2017).

[54] P. Mandal, R. K. Patel, D. Rout, R. Banerjee, R. Bag, K. Karmakar, A. Narayan, J. W. Freeland, S. Singh, and S. Middey, Giant orbital polarization of Ni^{2+} in a square planar environment, Phys. Rev. B **103**, L060504 (2021).

[55] I. Tsukada and S. Ono, Negative Hall coefficients of heavily overdoped $La_{2-x}Sr_xCuO_4$, Phys. Rev. B **74**, 134508 (2006).

[56] N. P. Armitage, P. Fournier, and R. L. Greene, Progress and perspectives on electron-doped cuprates, Rev. Mod. Phys. **82**, 2421 (2010).

[57] W. O. Wang, J. K. Ding, B. Moritz, E. W. Huang, and T. P. Devereaux, DC Hall coefficient of the strongly correlated Hubbard model, npj Quantum Mater. **5**, 51 (2020).